Title

Damage detection using the signal entropy of an ultrasonic sensor network

Journal

Smart Materials and Structures, 24(7)

ISSN

0964-1726

Authors

Rojas, E

Baltazar, A

Loh, KJ

Publication Date

2015-07-01

DOI

10.1088/0964-1726/24/7/075008

Peer reviewed

Damage detection using the signal entropy of an ultrasonic sensor network

E Rojas[1,3], A Baltazar[1,4] and K J Loh[2,5]

[1] Robotics and Advanced Manufacturing Program. Centro de Investigación y de Estudios Avanzados del Instituto Politécnico Nacional – Unidad Saltillo, Ramos Arizpe, Coahuila, 25903, México.
[2]Department of Civil & Environmental Engineering, University of California, Davis, CA 95616, USA.

[3] 05.erickrojas@gmail.com
[4] Corresponding author: arturo.baltazar@cinvestav.edu.mx
[5]kjloh@ucdavis.edu

Abstract. Piezoelectric ultrasonic sensors used to propagate guided waves can potentially be implemented to inspect large areas in engineering structures. However, the inherent dispersion and noise of guided acoustic signals, multiple echoes in the structure, as well as a lack of an approximate or exact model, limit their use as a continuous structural health monitoring system. In this work, the implementation of a network of piezoelectric sensors randomly placed on a plate-like structure to detect and locate artificial damage is studied. A network of macro fiber composite (MFC) sensors working in a pitch–catch configuration was set on an aluminum thin plate 1.9 mm in thickness. Signals were analyzed in the time-scale domain using the discrete wavelet transform. The objectives of this work were threefold, namely to first develop a damage index based on the entropy distribution using short time wavelet entropy (STWE) of the ultrasonic waves generated by a sensor network, second to determine the performance of an array of spare macro fiber composite (MFC) sensors to detect artificial damage, and third to implement a time-of-arrival (TOA) algorithm on the gathered signals for damage location of an artificial circular discontinuity. Our preliminary test results show that the proposed methodology provides sufficient information for damage detection, which, once combined with the TOA algorithm, allows localization of the damage.

Keywords: guided waves, TOA algorithms, sensor network, entropy.

1. INTRODUCTION

Civil, mechanical, aerospace, and naval structures, among others, could experience damage throughout their operational service lifetimes. Damage, if left undetected, could propagate and cause catastrophic failure. Therefore, the continuous monitoring of structural performance and the detection of

damage in a timely fashion becomes critical, whether it is to provide warning of pending structural collapse or to provide rich datasets for facilitating the making of informed decisions regarding repair. In particular, structural health monitoring (SHM) systems combine advanced sensor technology and algorithms to provide information to interrogate a structure's condition. As such, the data generated from monitoring structures can facilitate repair efforts and prevent catastrophic structural failure.

Among the plethora of sensor technologies in the market today or currently under development, piezoelectric sensors are commonly used for nondestructive evaluation to monitor the health conditions of engineering structures due to their ability to be simultaneously used as a transmitter and a receiver. For example, an array of piezoelectric sensors has been used for continuous monitoring on aircraft wings to detect and localize rivet-hole cracks (Zhao, et al., 2007). Other examples can be found in civil structures to detect damage on a bolt-joined steel plate and the presence of cracks in bridges (Park, et al., 2006). New developments in piezoelectric sensors to make them more cost/effective have been investigated. Nanocomposite piezoelectric sensors have been designed, studied, and proposed as potential sensors to detect cracks, corrosion and other aging effects in pipelines used by the gas and petroleum companies (Dodds, et al., 2013) (Meyers, et al., 2013).

Ultrasonic guided waves have been proposed as a technique for structural health monitoring (SHM) due to their high sensitivity to hidden defects and the ability of guided waves to travel long distances ((Rose, 1999); (Cheeke, 2002)). With the use of guided waves, the ability to monitor the health of the structure can be extended, as well as the size of the component being interrogated. However, structural conditions (shape, access, and size) of the object under evaluation, as well as noise, wave dispersion, and simultaneous generation of coupled vibrational modes, limit a broader use of guided waves.

Several techniques for guided wave characterization of defects using ultrasonics have been studied, such as single transducers (Ghosh, et al., 1998), phase array transducers (Wilcox, 2003), helicoidally propagation (Balvantin, et al., 2012); and tomography propagation (Malyarenko & Hinders, 2001). Some of these techniques have shown to be promising for damage detection. On the other hand, an array of ultrasonic sensors has been proposed as a plausible alternative for developing a continuous health monitoring system. An array of sensors (or sensor network) can be defined as a spatially distributed array of sensors designed to obtain measurements from the environment, thereby allowing it to obtain relevant information from the data gathered and to derive appropriate inferences from the information gained (Iyengar, et al., 1991). Sensor networks have been widely studied in research areas such as sensing, communication, and computing to improve detection, localization, tracking, and classification of targets (Moreno, et al., 2012) (Chee Yee & Srikanta , 2003) (Farrar, et al., 2011). Sensors can be spatially distributed to generate a network array in a pitch-catch configuration to interrogate the condition of the structure (Johnson, et al., 2004), which, when combined with algorithms to process the signals, can be used to detect damage in different types of structures ((Zhao, et al., 2007); (Ihn & Chang, 2004) (Michaels, 2008)). The use of sensor networks has been considered for SHM, because it provides high coverage with a relative small number of transducer elements (Flynn, et al., 2011).

A few techniques have been proposed to improve damage localization using algorithms based on time-of-arrival; Michaels & Michaels (2007a) proposed data fusion using time-of-arrival (TOA) algorithms of scattered signals to improve damage localization. Flynn et al. (2011) proposed a statistical method to evaluate localization performance of various algorithms based on TOA. Ihn & Chang (2008) proposed to preprocess the differenced signal using short-time Fourier transform (STFT) to obtain information in the time domain from the scattered signal and then apply it to the TOA algorithms.

Michaels & Michaels (2007b) suggested using the signal energy contained in a narrow time window of the scattered signal to minimize the effects of multiple patterns around sensor pairs.

The concept of entropy was introduced by Shannon (1948) as a quantitative criterion for analyzing probability and amount of information of any random variable distribution. Thus, entropy can be assumed to be an indicative of the degree of order of a complex signal. Typical non-stationary signals have high degrees of entropy because of their frequency changes through time. Time-evolving entropy can be measured using a windowed technique into the wavelet coefficients provided by the discrete wavelet transform to search for sudden changes of energy within the signal. A non-stationary guided wave signal is expected to vary its energy distribution through time as well as frequency and then the change of energy distribution will lead to a disorder of the signal.

Wavelet entropy was used to detect and identify the transmission line fault (El Safty & El-Zonkoly, 2009). Rosso *et al* (2001) proposed a time evolution wavelet entropy method in electro-encephalographic signals to find key points to identify a signal that indicates if an individual has his eyes closed or open. The concept wavelet entropy was also used in (Passoni, et al., 2005) to evaluate dynamic biospeckle images and characterize transient processes such as drying of paint. Yan et al., (2009) developed a technique for damage identification using Lamb waves called frequency slice wavelet transform. In this work we extend, the concept of wavelet entropy to the field of structural health monitoring (SHM) to work in conjunction with TOA with the purpose of developing a method capable of detecting small changes in non-stationary signals contaminated with noise.

As it can be seen, the basic idea behind the application of an array of sensors and its further post-processing is that by combining information from the sensors, the probability for damage localization could increase. In this work, time evolution of wavelet entropy is incorporated into a time of arrival algorithm using data generated from guided waves propagated in a thin plate by an array of sensors to improve damage identification. The objectives of this work are: first, to discuss the implementation of the proposed short time evolution entropy of wavelet transform (STWE) into time of flight (TOA) algorithms; second, to carry out experiments on an aluminum plate with artificial damage using an array of spare macro fiber composite (MFC) sensors; third, to implement the time evolution entropy of wavelet transform of the guided waves obtained from the experiments implementing modification of a time of arrival (TOA) using STWE.

The paper outline starts with a description of the STWE and TOA algorithms. Then, the performance of the proposed TOA algorithm with STWE technique is proved with synthetic signals. The proposed methodology is applied on experimental signals obtained from Lamb waves propagated in a thin aluminum plate. Finally, in the last section, conclusions and future work are presented.

2. SHORT TIME WAVELET ENTROPY (STWE)

Wavelet analysis is a technique of signal processing that, in contrast with short time Fourier transform (STFT), characterizes a signal at a certain time window Δt by performing a multi-scale algorithm (Stark, 2005). The signal is simultaneously analyzed in time and frequency to transform it into a representation which either makes certain features of the original signal more easily studied or enables the original data set to be described more efficiently.

The discrete wavelet transform of a continuous signal, $x(t)$, using discrete dyadic wavelets can be expressed as (Addison, 2002):

$$T_{j,k} = \frac{1}{\sqrt{2^j}} \int_{-\infty}^{\infty} x(t)\psi(2^{-j}t - k)dt \,, \tag{1}$$

or as the inner product:

$$T_{j,k} = \left\langle x, \psi_{j,k} \right\rangle, \tag{2}$$

where $T_{j,k}$ are known as wavelet coefficients or details coefficients, j is the resolution level, k are each of the elements in the time series, and $\psi_{j,k}(t)$ is the wavelet function. The discrete wavelet transform (DWT) results in discrete blocks of wavelet coefficients with a number of elements that reduces as j increases (Torrence & Compo, 1998) .

It is known that by using a discrete wavelet transform (DWT) a signal $x(t)$ can be decomposed in a combined series expansion of approximation coefficients and wavelet coefficients:

$$x(t) = a_{j_0,k}(t) + \sum_{j=-\infty}^{j_0} d_{j,k}(t) \,. \tag{3}$$

Thus, for each of the j levels of the decomposition, the details and the approximation coefficients are:

$$d_{j,k}(t) = \sum_{k=-\infty}^{\infty} T_{j,k}\, \psi_{j,k}(t) \,, \tag{4a}$$

$$a_{j_0,k}(t) = \sum_{k=-\infty}^{\infty} a_{j,k}\, \phi_{j,k}(t), \tag{4b}$$

where $\phi_{j_0,k}(t)$ is the scaling function defined as:

$$\phi_{j,k}(t) = 2^{-j/2}\phi(2^{-j}t - k) \,. \tag{5}$$

Equations (4) allow an inspection of the signal filtered by different frequency bands called reconstructed wavelet coefficients. Thus, DWT is commonly used to remove noise in a focused frequency band.

The wavelet energy at each resolution reconstructed level is given by:

$$E_j = \sum_k \left| d_{j,k}(t) \right|^2. \tag{6}$$

Thus, for the entire signal, the total energy is:

$$E_{tot} = \sum_j E_j \,. \tag{7}$$

Using (6) and (7), it is possible to assign a degree of occurrence equal to the normalized value of the energy to obtain the probability distribution of the wavelet energy corresponding to the resolution level j.

$$p_j = \frac{E_j}{E_{tot}}, \tag{8}$$

where from probability theory $\Sigma p_j = 1$.

The distribution p_j gives a suitable tool for detecting and characterizing the signal energy distribution in the time and frequency domains. It can also be used to compute the entropy, which is a concept introduced by Shannon ((Shannon, 1948), (Rosso, et al., 2001)). The entropy is a quantitative criterion for analyzing probability and the amount of disorder of any distribution. The entropy is defined by:

$$H = -\sum_j p_j \ln(p_j). \tag{9}$$

This can be considered a measure of the average uncertainty of a random variable (wavelet energy at level *j*). The wavelet energy entropy can be applied to detect events that modify the energy distribution of the signal.

To be specific, for a non-stationary signal, the frequency content is a function of time. As shown in Figure 1 , to study its temporal evolution of entropy, the signal is divided in *i* intervals of windows length *L* (*i* = 1, 2,…, *Nt*, with *Nt = M/L, M* is the total sample time) (Rosso, et al., 2001). At each *j* (*j*=1, 2, ..., *N*, *N* is the number of levels) level of the discrete wavelet transform in a time window of length *L*, the energy can be obtained using (10) (figure 1b).

$$E_j^i = \sum_{k=(i-1)L+1}^{iL} |d_{j,k}|^2, \tag{10}$$

where *d* is the signal detail at the scale *j*, and *k* is each sampled time. Equation (10) shows the energy distribution of each reconstructed level of the wavelet transform (figure 1c). This representation of energy in time domain allows the use of the energy time of flight, filtered with the wavelet transform.

The sum of energies in a window time at each resolution level is the total energy given by:

$$E_{tot}^i = \sum_j E_j^i. \tag{11}$$

The changes in signal energy are represented by the probability distribution. Thus, the time evolution of wavelet energy distribution is:

$$p_j^i = \frac{E_j^i}{E_{tot}^i}. \tag{12}$$

Then, with the probability obtained at each window in each level, it is possible to determine changes in signal but now in terms of entropy in the time-domain using:

$$H^i = -\sum_j p_j^i \ln(p_j^i), \tag{13}$$

where *i* represents the window interval in which entropy is calculated.

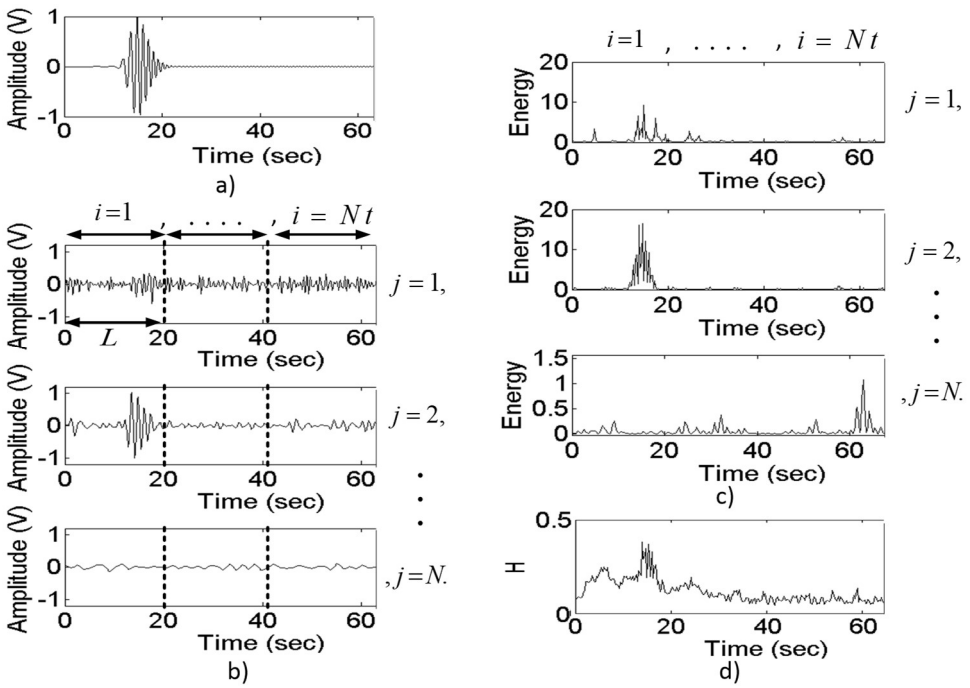

Figure 1. Post-processing of a signal with the proposed short time wavelet transform (STWT). a) Simulated signal, b) DWT of the signal, c) time energy distribution at each level of DWT and d) time evolution entropy. Dashed lines represent the time window length (L), i is the window interval, and j is the resolution level.

Thus, the short time wavelet entropy (STWE) is obtained with (13), it gives the signal entropy change as a function of time at each window where the energy is calculated (see figure 1d). In general, the entropy of any random variable depends only on its probability distribution and not on the values of the variables. Therefore, it is expected that the signal amplitude will not influence the estimated entropy.

3. DAMAGE LOCALIZATION ALGORITHMS BASED ON ENTROPY

Two algorithms, TOA and time difference of arrival (TDOA), for damage localization have been studied recently in several works (i.e., (Michaels, 2008); (Flynn, et al., 2011); (Hyung Keun, et al., 2010); (Lee & Rizos, 2008)). These algorithms use the estimation of time-of-flight of a scattered signal for determining a possible damage location. The TOA algorithm is based on the sum of amplitudes calculated from the difference between a base signal and the signal obtained for the damage case. TDOA uses the cross-correlation between the differenced signals (base and damage signals) obtained from each receiver pair sensors, and makes use of this statistical tool to account for the uncertainty in the measurements; thus, the technique requires slightly more computational effort than TOA, which only requires the determination of the amplitude of a signal.

The potential uses of these algorithms have been investigated in other studies (Lee & Rizos, 2008). However, the presence of wave dispersion, mode conversion, signal noise, and attenuation in the propagated wave packets limit their performance. The generation of artifact patterns in the reconstructed image reduces the probability (and accuracy) of damage detection. To overcome this problem, this study

investigated pre-processing the signal with the proposed STWE technique applied on the difference signals prior to the implementation of the TOA algorithm. It is hypothesized that this technique could yield better performance with noisy signals and enhance computational efficiency.

TOA algorithm (Michaels, et al., 2008) uses a minimum of two sensors to locate the damage, that is, one acts as a transmitter and the other as a receiver. Therefore, if there is damage located at point (*x, y*), the time of flight of the scattered signal can be estimated as follows:

$$t_{ab}(x,y) = \frac{\sqrt{(x_a - x)^2 + (y_a - y)^2} + \sqrt{(x_b - x)^2 + (y_b - y)^2}}{C_g}, \tag{14}$$

where x_a, y_a are the transmitter cordinates; x_b , y_b are the receiver cordinates, and the amplitude of the signal is taken at the (*x, y*) location; C_g is the group velocity of the carrier frequency.

A schematic illustrating the TOA algorithm is shown in figure 2, the ellipse is generated using the time of flight of the scattered signal, and it indicates all possible damage locations using only two sensors. Also the scheme shows the direct wave generated by the sensor and the scattered wave generated by the damage.

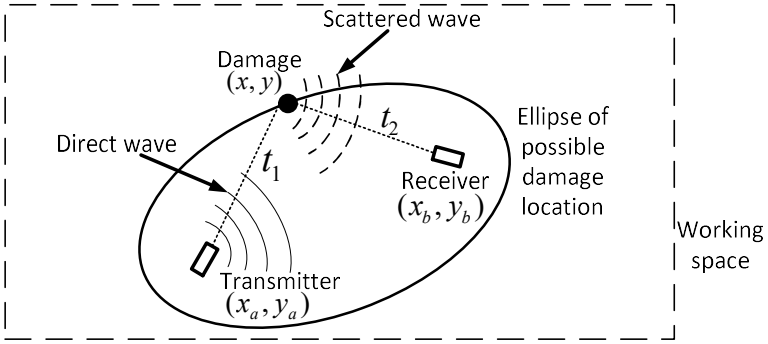

Figure 2. Schematic of a sensor network spatially distributed; t_1 and t_2 indicate the time of flight from transmitter-damage-receiver path.

In the original algorithm, damage localization is obtained by taking the sum of the amplitude at time t_{ab}. This generates an ellipse of maximum probability for damage location around the paired sensors. Using STWE, the damage localization at point (*x, y*) is obtained by the sum of the entropy′s ampitude as follows:

$$I(x,y) = \sum_{a=1}^{N} \sum_{b=2}^{N} D^i(t_{ab}(x,y)), \qquad i = 1,2,...,Nt, \tag{15}$$

where $D^i = H_d^i - H_s^i$, is the difference in entropy at time location $t_{ab}(x,y)$, and H_d^i and H_s^i are the entropies of the signal with damage and the signal without damage respectively.

The block diagram in figure 3 summarizes the steps for the implementation of STWE and TOA algorithm for damage localization.

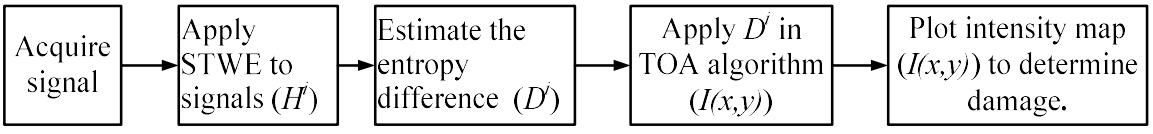

Figure 3. Block diagram for damage localization using TOA algorithm and STWE technique.

4. NUMERICAL RESULTS

Numerical calculations were performed simulating a sensor array in a test space (250 x 250 unit cells) and a circular discontinuity with no dimensions set at the (150, 200) location (figure 5). Time-of-flight is predicted by assuming a straight propagation without attenuation from actuator to the discontinuity to the receiver, so as to simulate the scattered signal generated from the simulated damage. The propagated wave was simulated using a synthetic Gaussian modulated sine wave with dispersion (wave number dependence frequency) and white noise using:

$$A(x,t) = \exp[-\frac{1}{2}\left(\frac{x - x_0 - C_g t}{\sqrt{\sigma^2 - it\Gamma}}\right)^2]\exp(ik_0(x - C_g t))\exp(ik_0 t(C_g - C_p)) + \varepsilon \quad (16)$$

where x is the spatial location of the wave, x_0 is the spatial reference (center of the modulated Gaussian function), k_0 is the wavenumber estimated at the carrier frequency ω_o, C_g is the group velocity, C_p is the phase velocity at ω_o, σ^2 is the width of the wave packet at t=0, and ε accounts for Gaussian white noise. The first exponential term in (16) shows the dispersion effect by increasing the width of the wave packet as a function of time. The relation between wavenumber and frequency used here is given by:

$$\omega = C_p k^2 \quad (17)$$

where ω is the angular frequency, and k the wavenumber.

Figure 4a shows synthetic signals generated using (16). The signal is then buried in Gaussian noise (figure 4b) using a signal-to-noise ratio (SNR) of 5. Even when SNR is this low, the STWE (figure 4c) is capable of identify the location of the original signal.

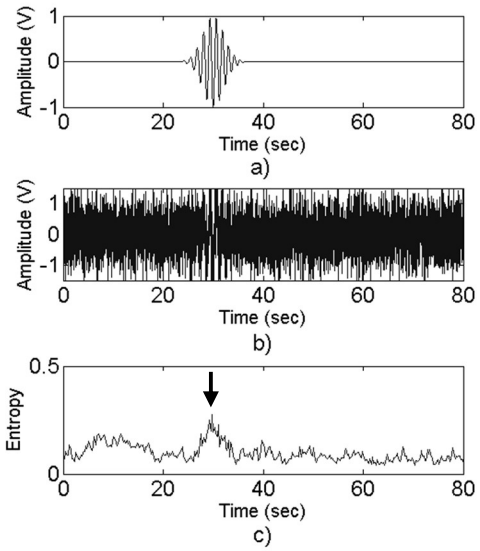

Figure 4. a) Propagated pulse; b) propagated pulse buried in noise; c) STWE of the signal. The black arrow indicates the location where the change in entropy corresponding to the pulse occurs.

The dashed lines in figure 5a indicates the spatially analyzed area in which four sensor locations each generated one ellipse for each pair of sensors. The results of the TOA algorithm using direct time analysis of the synthetic signals are given in figure 5b. It can be observed that noise added to the signal (SNR=5) adversely affects the localization of damage. In addition, wave dispersion prompts TOA to generate multiple ellipses around each paired sensor, thereby making it difficult to identify a possible damage location (*i.e.*, black arrow in this figure). The TOA algorithm is based on the sum of values that represent the signal at a specific time; thus, changes of energy (dispersion) at different points in time would increase the uncertainty in damage location by generating multiple intersections of the ellipses.

In figure 5c, the result of STWE implementation is given. A better localization of the damage (figure 5c) using the modified TOA algorithm (15) was obtained even with a high noise level (SNR=5). STWE improves the results since it acts as a natural band-pass filter with high sensitivity to small changes in signal energy. The DWT has the characteristic of energy preservation (Addison, 2002), and STWE takes advantage of this characteristic to determine energy changes in the signal. Thus, damage localization using TOA is based on the entropy summation and not on the signal amplitude summation.

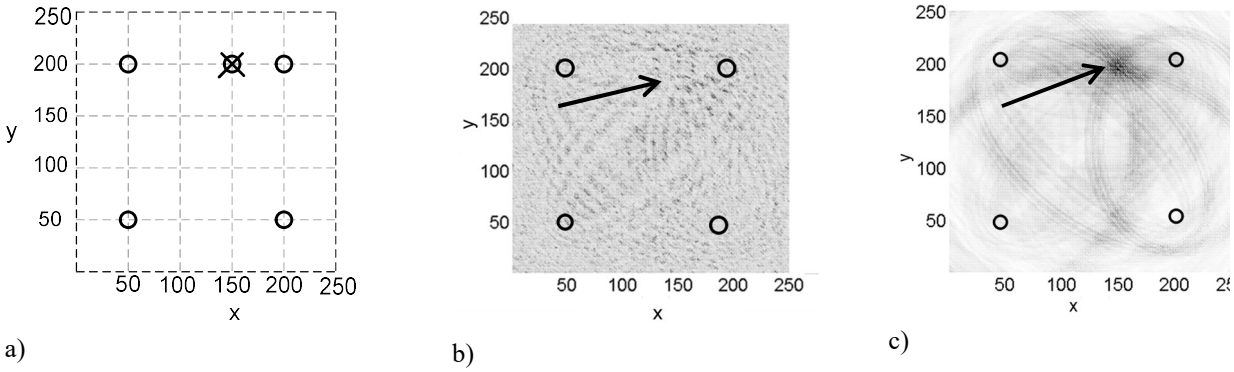

Figure 5. a) Working space for simulations; black circles represent the position of the sensors, and the crossed circle is the simulated discontinuity; b) TOA results using noisy and dispersive synthetic signal; c) TOA result using the pre-processed signal with STWE; black arrow indicates the actual damage localization.

5. EXPERIMENTAL SET UP

To test the performance of the proposed algorithm, macro fiber composite (model MFC-M2814) sensors manufactured by Smart Material Inc., with an active area of 28 mm *x* 14 mm and a bandwidth of 750 kHz, were used. The typical physical structure of an MFC sensor is formed by rectangular piezoceramic fibers locked in an epoxy matrix and sandwiched between two arrays of integrated electrodes (see for example (Eaton, et al., 2009) for details). The rectangular piezoceramic fibers are arranged in a regular spacing and precise parallel alignment to form the MFC transducer. The fibers are sandwiched by polyimide films on the top and bottom. When an electric field is applied to the transducer, the unique electrode pattern formed by the piezoceramic fibers allows the MFC transducers to generate corresponding d_{33}-displacements. The amplitude of the signal depends on the polarization direction of the

fibers and the electrodes. These features promote higher sensitivity to in-plane displacement in the MFC sensors as compared with PZT sensors, which are typically more sensitive to out-of-plane displacements.

Several tests to identify the vibrational modes generated by the proposed sensors were carried out. Then, the results were compared with typical commercial piezoelectric (PZT) transducers, 12.25 mm in diameter and a center frequency of 1 MHz. Two MFC sensors, a transmitter and a receiver, were located at a distance of 200 mm between each other, and a six-cycle tone burst input signal with a carrier frequency of 750 kHz was used. A similar approach was performed but by substituting the MFC sensor with two PZT transducers while keeping the same separation distance but using instead 260 kHz as the carrier frequency of the six-cycle tone burst. These frequencies are in a range where the dispersion of the A0 and S0 modes (figure 6a) is reduced to a minimum. Also, the in-plane and out-of-plane displacements (figure 6b) at these frequencies exhibit good matching between the MFC and PZT sensors.

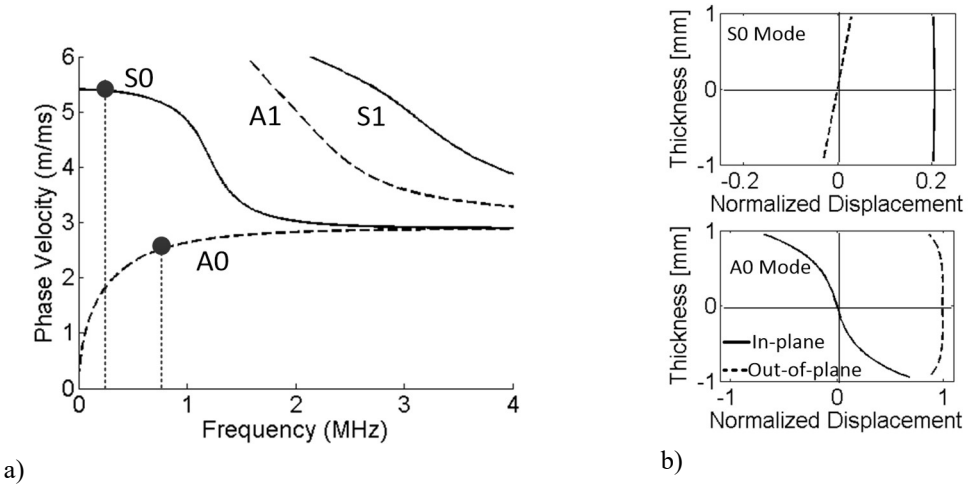

a) b)

Figure 6. a) Phase dispersion curves for an aluminum plate with 1.9 mm in thickness; b) corresponding in-plane and out-of-plane displacements for S0 (260 kHz) and A0 (750 kHz) respectively.

Identification of the vibrational mode using each of the gathered signals was performed experimentally by post-processing the signals using the short-time Fourier transform. Time-domain signals (as measured by the sensor) and their corresponding STFT, as well as theoretical Lamb's wave predictions (solid and dashed lines), are shown in figure 7. It can be seen that the ability to detect the A0 vibrational mode is enhanced when using MFCs due to large in-plane displacements (figure 6b).

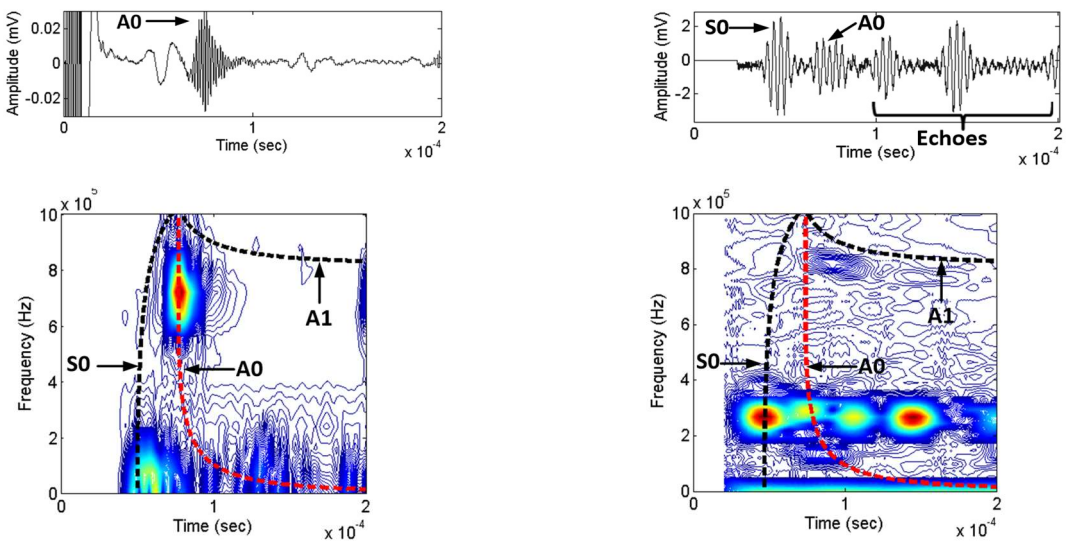

Figure 7. a) Time domain record and corresponding STFT of received signal with a) MFC; b) PZT sensors (dashed lines are theoretical dispersion curves of group velocity).

The attenuation of the S0 and A0 modes measured with the PZT and MFC sensors respectively were determined by taking the signals at distances ranging from 50 mm up to a total distance of 250 mm. The results are given in figure 8, where the amplitude of the received mode was estimated from the STFT. A monotonic reduction of the amplitude of the two vibrational modes is observed; a least-squared fitting to an exponential model gives an attenuation coefficient equal to about 0.04 dB/mm for both A0 mode and S0. This value is close to that reported in the literature and indicates that monitoring of the vibrational modes up to a 0.4 m distance (considering the distance among the sensors in the experimental setup) should be feasible.

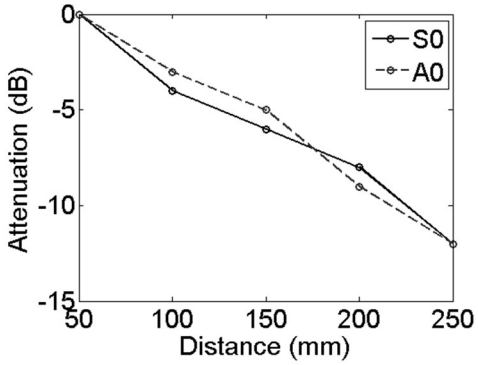

Figure 8. Signal attenuation measured at intervals of 50 mm.

The directionality sensitivity is also a concern with MFC sensors (Eaton, et al., 2009). To characterize the response of a typical MFC sensor, a set of preliminary tests was carried out on a thin aluminum plate with dimensions of 600 x 600 mm^2 and 1.9 mm in thickness. The transmitter was fixed at the center of the plate, while the receiver sensors were placed in a circular pattern that surrounded the

actuator. A total of eight signals were taken at interval angles of 45°, as shown in figure 9a. At each location, a receiver sensor was attached to the aluminum plate using simple double-sided tape. In figure 9b, the amplitude energy of the A0 vibrational mode measured on the STFT map as a function of the location angle is given. At 90° and 270°, the energy response is higher than for other angles. This can be explained by the fact that the MFC sensors (d_{33}-type) generated mainly in-plane displacements along the piezoceramic fiber (Tolliver, et al., 2013). As a result, when the piezoceramic fibers of both sensors are aligned in the same direction, MFC sensors exhibit better performance and sensitivity due to its polarization direction. This indicates that the relative directionality of the MFC sensors with respect to each other could affect their performance and have a lower sensitivity than nominally omnidirectional PZT transducers (figure 9c).

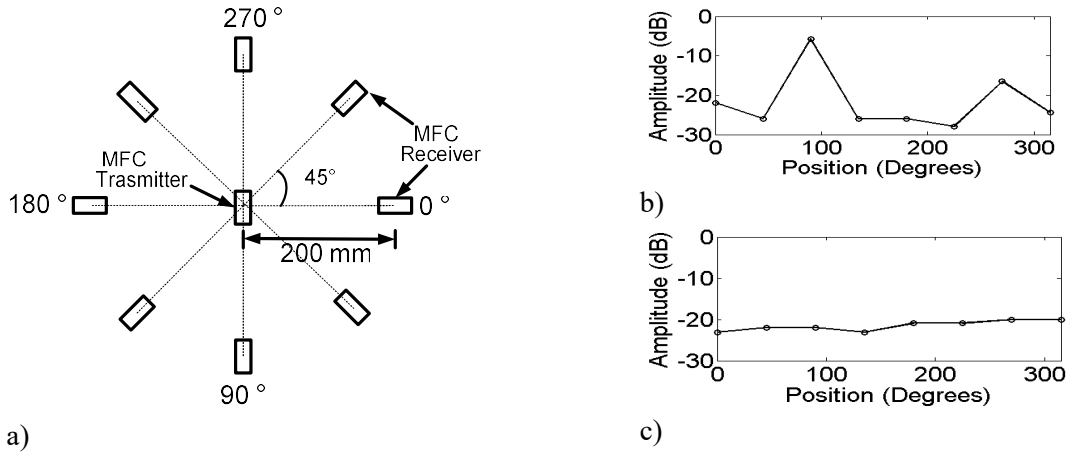

Figure 9. a) Sensor position scheme to evaluate omnidirectional sensitivity of MFC sensors; b) and c) are the results of maximum amplitudes at 45° intervals with MFC and PZT sensors respectively.

The implementation of the STWE technique in a TOA algorithm for damage detection was carried out in the same aluminum plate that was used for the sensors' characterization; however, a small 6.3 mm in diameter through-hole was drilled in the plate to simulate damage. A symlet 4 wavelet was used to perform the analysis in STWE; as described in Ibañez et al. (2015) for the analysis with ultrasonic guided waves, it exhibits a good cross-correlation criteria between the original signal and its approximation coefficients.

For the experiments, the sensors were placed in an area in the proximity of the center of the aluminum plate to minimize the echoes from plate's edges. As part of the implementation of the proposed TOA algorithm, each sensor was set to work as transmitter and receiver. The tone burst was generated by a function generator (Agilent 33220A), then the signal was gathered by a broadband receiver (Ritec Broadband BR-640A) and averaged (64 times) with an oscilloscope (Tektronix TDS 1012). Figure 10 shows a scheme of the localization of sensors and the equipment used in the experimental tests.

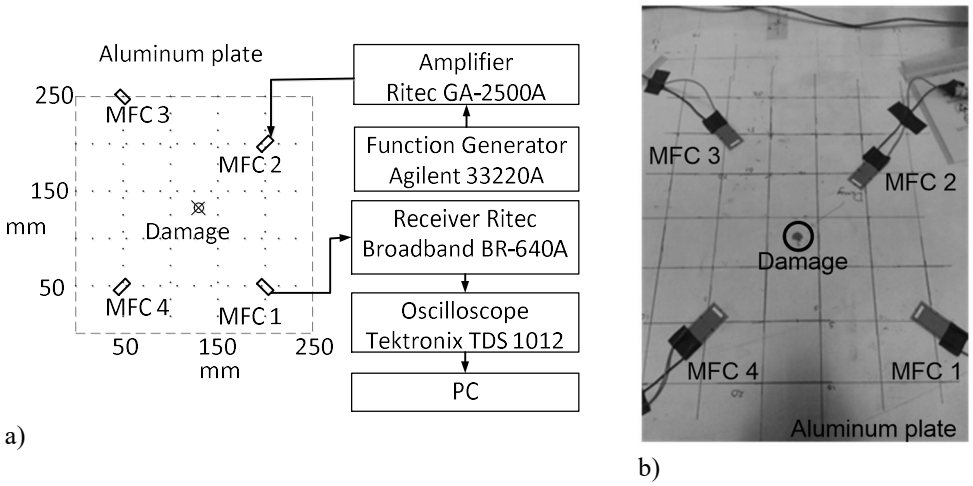

Figure 10. a) MFC sensor array setup; b) photograph of the actual MFC sensor array and damage.

6. RESULTS AND DISCUSSION

As depicted in figure 10b, there are slight variations in distances and orientations among the sensors, and the discontinuity that could have an effect on the collected signals. As shown for two MFC sensors in a pitch-catch configuration, the sensor could be receiving both, the direct wave and a secondary scattered signal. In the absence of a discontinuity, only the sensor will receive the direct wave, and ideally, the difference between the signal with and without damage will approach zero. Thus, according to the proposed TOA algorithm, the scattered signal information will create an ellipses pattern for each transmitter/receiver combination. As discussed previously, due to the directionality of MFC sensors, the scattered wave can be more readily detected if it arrives with a collinear direction between the scattered wave direction and the receiver.

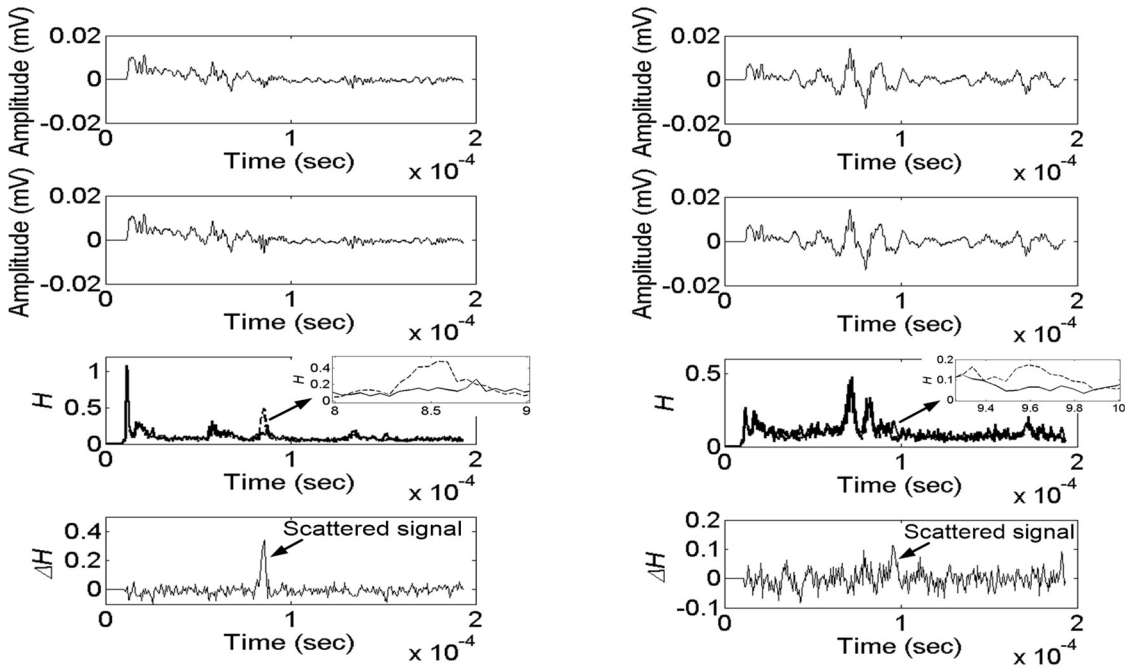

Figure 11. Results found for the STWE analysis, the first three rows of plots show the base, damaged and the entropy from the first two signals, and at the bottom row is the difference between signal entropies. Signals taken from: a) MFC1 to MFC2 (actuator and sensor respectively); b) MFC1 to MFC4 sensor (see figure 10a). Black arrow indicates a change in signal related to the damage. Dashed line is the entropy from signal with damage.

In figure 11, typical results of signal processing obtained with the array of MFC sensors described in figure 10 are presented. These were obtained from two possible combinations, namely MFC1-MFC2 and MFC1-MFC4 transmitter/receiver combinations. Table 1 gives the predicted and the experimental TOF estimations based on the theoretical dispersion curves and short time Fourier transform (STFT) of the obtained signal. The experimental TOF was measured on STFT maps since it was very difficult in some cases to detect the scatter signal on the time traces. The TOF estimated and measured values (STFT) are about 5 to 7 μs off, but they still provide information to define a time window where the direct wave and scattered signal are expected to arrive.

Table 1. Time of flight (TOF) of all MFC actuator/sensor combination shown in figure 10.

Actuator-receiver	TOF of direct wave theoretical (experimental) μs	TOF of Scattered signal theoretical (experimental) μs
MFC1-MFC2	57 (62)	85 (86)
MFC1-MFC3	100(97)	100(not detected)
MFC1-MFC4	71 (76)	100 (95)
MFC2-MFC3	57(not detected)	101(not detected)
MFC2-MFC4	75(78)	75(79)
MFC3-MFC4	71(73)	91(93)

The time-domain analysis (first two rows in previous figure) shows small differences between the damaged and undamaged conditions. For the signal from MFC1-MFC2, a signal related to the scattered signal from the defect is found at about 85 μs. For MFC1-MFC4, the signal traces are practically similar, with no noticeable signal of the scattered wave at the predicted time (~100 μs), as is indicated in table 1.

In the third row in figure 11 the STWE is applied to the time-domain signals; a comparison between results for the two signals is presented. The entropy distributions are basically the same with only a small variation at 86 μs for MFC1-MFC2 and 95 μs for MFC1-MFC4. A zoom window where the entropy distribution is modified by the scattered signal is also shown. Then, the entropy distribution of the base is subtracted from the damage and presented in the fourth row of this figure. After the subtraction operation is performed, a possible indication of the scattered signal from the artificial damage is revealed. Even for the MFC1-MFC4 combination, there is a small detectable indication apparently related to the scattered signal at the expected time, which is indicated in table 1.

Once the difference of the entropy distribution for each combination of transmitter-receiver is estimated, the TOA algorithm described in previous section was implemented. The results are given in figure 12. The proposed TOA algorithm was compared with typical TOA results using only the amplitude difference of the raw signals in figure 12a (typical approach). In both cases, the generated ellipses showed high probability of damage located at their periphery; the intersection among the ellipse locates the discontinuity. Here, only three ellipses are formed indicating that the differenced signal, or entropy, for some of the sensor combinations have a small amplitude contribution, which is below the noise level to generate an ellipse indication.

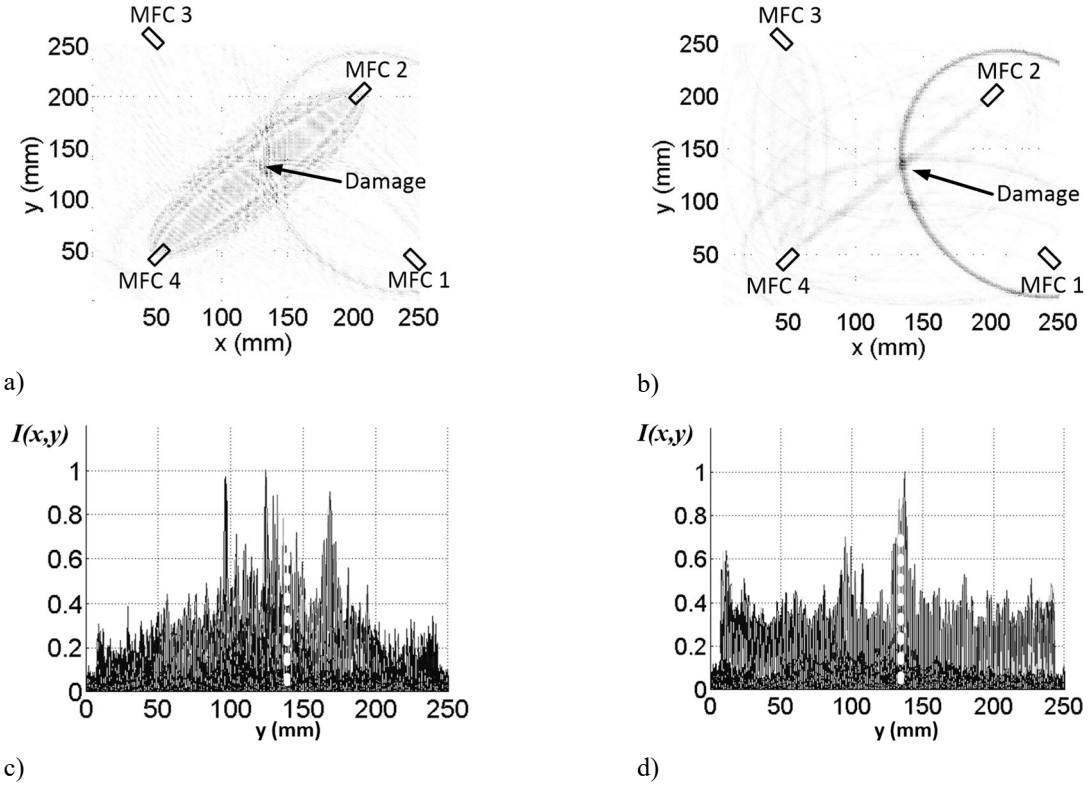

Figure 12. TOA results using the signals a) without any prepossessing; b) using STWE technique; c) and d) are a side view of plots. The dashed white lines indicate actual damage localization in the y-direction.

Therefore, the proposed STWE technique allows a clearer indication of the probably location of the artificial damage than the results using the raw signals. The result using raw signals are mainly the results of noise and the dispersion of the received signals. The actual damage location is at the (130 mm, 130 mm) position. Figures 12c and d show a cross-section from the maps generated with TOA algorithm for damage localization; it is clear that, for the results of the proposed TOA (figure 12d), the largest amplitude is correctly located at the expected determined location.

7. CONCLUSIONS

The numerical results show that that the proposed time-of-arrival (TOA) algorithm based on the short time windowed entropy technique (STWE) performed better than the typical TOA algorithm under test conditions with small dispersion and noise. The experimental tests were carried out using macro fiber composite sensors (MFC). The sensors were characterized, and their performance was compared with commercial (PZT) transducers. It was found that the directionality of the MFC sensors is a major drawback for their implementation. In the tests described in this study, it was assumed that the area of high probability of damage was known and that it was located at the center of the aluminum test plate. The sensors were placed around a circle forming a diameter of 250 mm with a small through-hole (6.3 mm in diameter) made near the center to simulate damage. The results showed that the proposed TOA is able to correctly locate the artificial damage even when using just a few sensors (*i.e.*, four MFC sensors) with almost no additional computational effort (*i.e.*, when compared to a TOA algorithm using only the arrival time). Future work will entail optimizing the number, topology of the sensors as well as the development of a new damage index based on relative entropy, which could allow the practical application of the proposed technique for monitoring and detecting damage occurring in actual engineering structures.

8. ACKNOWLEDGMENTS

The authors thank CONACYT for providing financial support for Erick Rojas enrolled in the Ph.D. program at Cinvestav. The authors also gratefully acknowledge UC MEXUS-CONACYT (grant no. CN 11-510) and the 2014 UC MEXUS Small Grant for the financial support of this research.

9. References

Addison, P. S., 2002. *The Illustrated Wavelet Transform Handbook: Introductory Theory and Applications in Science, Engineering, Medicine and Finance.* First ed. UK: CRC Press .

Balvantin, A., Baltazar, A. & Kim, J., 2012. A study of helical Lamb wave propagation on two hollow cylinders with imperfect contact conditions. *AIP Conference Proceedings,* 1511(1), pp. 67-74.

Chee Yee, C. & Srikanta , K., 2003. Sensor Networks: Evolution, Opportunities, and Challenges. *Proceedings of the IEEE,* 91(8), pp. 1247-1256.

Cheeke, J. D. N., 2002. *Fundamentals and Applications of Ultrasonic Waves.* First ed. Montreal: CRC Press LLC.

Dodds, J. S., Meyers, F. N. & Loh, K. J., 2013. Piezoelectric nanocomposite sensors assembled using zinc oxide nanoparticles and poly (vinylidene fluoride). *Smart Structures and Systems,* 12(1), pp. 55-71.

Eaton, M. et al., 2009. Use of Macro Fibre Composite Transducers as AcousticUse of Macro Fibre Composite Transducers as Acoustic Emission Sensors. *Remote Sensing,* pp. 68-79.

El Safty, S. & El-Zonkoly, A., 2009. Applying wavelet entropy principle in fault classification. *International Journal of Electrical Power & Energy Systems,* Vol. 31(10), pp. pp.604-607.

Farrar, C. R., Park, G. & Todd, M., 2011. Sensing Network Paradigms for Structural Health Monitoring. *New Developments in Sensing Technology for Structural Health Monitoring Lecture Notes in Electrical Engineering,* Volume 96, pp. 137-157.

Flynn, E. B. et al., 2011. Maximum-likelihood estimation of damage location in guided-wave structural health monitoring. *Proc. R. Soc. A,* Volume 467, p. 2575–2596.

Ghosh, T., Kundu, T. & Karpur, T., 1998. Efficient use of Lamb modes for detecting defects in large plates. *Ultrasonics,* 36(7), pp. 791-801.

Hyung Keun, L., Hee Sung, K., Ju Young , S. & Moon Beom, H., 2010. Analytic equivalence of iterated TOA and TDOA techniques under structured measurement characteristics. *Multidimensional Systems and Signal Processing,* 22(4), pp. 361-377.

Ibáñez , F., Baltazar, A. & Mijarez, R., 2015. Detection of damage in multiwire cables based on wavelet entropy evolution. To be published in *Smart Materials and Structures.*

Ihn, J. B. & Chang, F. K., 2004. Detection and monitoring of hidden fatigue crack growth using a built-in piezoelectric sensor/actuator network: II. Validation using riveted joints and repair patches. *Smart Mater. Struct.,* 13(3), pp. 621-630.

Ihn, J. & Chang, F., 2008. Pitch-catch Active Sensing Methods in Structural Health Monitoring for Aircraft Structures. *Structural Health Monitoring,* 7(1), pp. 5-19.

Iyengar, S. S., Kashyap, R. L. & Madan, R. N., 1991. Distributed sensor networks - Introduction to the special section. *IEEE Transactions on Systems, Man, and Cybernetics,* 21(5), pp. 1027-1030.

Johnson, T. J., Brown, R. L., Adams, D. E. & Schiefer, M., 2004. Distributed structural health monitoring with a smart sensor array. *Mechanical Systems and Signal Processing,* 18(3), p. 555–572.

Lee, H. K. & Rizos, C., 2008. Position-domain hatch filter for kinematic differential GPS/GNSS.. *IEEE Transactions on Aerospace and Electronic Systems,* pp. 30-40.

Malyarenko, E. V. & Hinders, M. K., 2001. Ultrasonic Lamb wave diffraction tomography. *Ultrasonics,* 39(4), pp. 269-281.

Meyers, F. N., Loh, K. J., Dodds, J. S. & Baltazar, A., 2013. Active sensing and damage detection using zinc oxide-based nanocomposites. *Nanotechnology,* Volume 24, pp. 1-10.

Michaels, J. E., 2008. Effectiveness of in situ damage localization methods using sparse ultrasonic sensor arrays. *Health Monitoring of Structural and Biological Systems,* Volume 6935, pp. 1-12.

Michaels, J. E., Croxford, A. J. & Wilcox, P. D., 2008. Imaging algorithms for locating damage via in situ ultrasonic sensors. *IEEE Sensors Applications Symposium,* pp. 63-67.

Michaels, J. E. & Michaels, T. E., 2007b. Damage localization in inhomogeneous plates using a sparse array of ultrasonic transducers. *Review of progress in cuantitative nondestructive evaluation,* Volume 26, p. 846–853.

Michaels, J. E. & Michaels, T. E., 2007a. Guided wave signal processing and image fusion for in situ damage localization in plates. *Wave Motion,* 44(6), pp. 482-492.

Moreno, M. V. et al., 2012. Multi-Sensor Multi-Target Tracking for Infrastructure Protection. *European Intelligence and Security Informatics Conference,* pp. 317-322.

Park, S., Yun, C.-B., Roh, Y. & Lee, J.-J., 2006. PZT-based active damage detection techniques for steel bridge components. *Smart Mater. Struct.,* 15(4), pp. 957-966.

Passoni, I. et al., 2005. Dynamic speckle processing using wavelets based entropy. *Optics Communications,* Vol.246 (1-3), pp. pp.219-228.

Rose, J. L., 1999. *Ultrasonic waves in solid media.* First ed. Cambridge: Cambridge University Press.

Rosso, O. et al., 2001. Wavelet Entropy: a new tool for analysis of short duration brain electrical signals. *Journal of Neuroscience Methods,* 105(1), p. 65–75.

Shannon, C., 1948. A Mathematical Theory of Communication. *The Bell System Technical Journal,* Volume 27, pp. 379-423,623-656.

Stark, H.-G., 2005. Wavelets and Signal Processing. An Application-Based Introduction. *Springer.*

Tolliver, L., Xu, T.-B. & Jiang, X., 2013. Finite element analysis of the piezoelectric stacked-HYBATS transducer. *Smart Mater. Struct.,* 22(3), pp. 1-11.

Torrence, C. & Compo, G. P., 1998. A practical guide to wavelet analysis. *Bulletin of the American Meteorological Society,* 79(1), pp. 61-78.

Wilcox, P., 2003. Omni-directional guided wave transducer arrays for the rapid inspection of large areas of plate structures. *Ferroelectr. Freq. Control,* 50(6), p. 699–709.

Yan, Z., Miyamoto, A. & Jiang, Z., 2009. Frequency slice wavelet trasform for transient vibration response analysis. *Mechanical systems and signal processing,* Volume 23, pp. 1474-1489.

Zhao, X., Gao, H. & Zhan, G., 2007. Active health monitoring of an aircraft wing with embedded piezoelectric sensor/actuator network: I. Defect detection, localization and growth monitoring. *Smart Mater. Struct.,* 16(4), pp. 1208-1217.